Werk

Jahr: 1975
Kollektion: fid.geo
Signatur: 8 Z NAT 2148:41
Digitalisiert: Niedersächsische Staats- und Universitätsbibliothek Göttingen
Werk Id: PPN1015067948_0041
PURL: http://resolver.sub.uni-goettingen.de/purl?PPN1015067948_0041

LOG Id: LOG_0018
LOG Titel: Crustal structure and P-Wave travel time anomalies at NORSAR
LOG Typ: article

Übergeordnetes Werk

Werk Id: PPN1015067948
PURL: http://resolver.sub.uni-goettingen.de/purl?PPN1015067948
OPAC: http://opac.sub.uni-goettingen.de/DB=1/PPN?PPN=1015067948

Contact

Niedersächsische Staats- und Universitätsbibliothek Göttingen
Georg-August-Universität Göttingen
Platz der Göttinger Sieben 1
37073 Göttingen
Germany
Email: gdz@sub.uni-goettingen.de

J. Geophys. 41, 71–84, 1975

Crustal Structure and *P*-Wave Travel Time Anomalies at NORSAR

K. A. Berteussen

NORSAR, Kjeller

Received July 12, 1974

Abstract. Deviations from theoretical, expected travel times are observed for *P* signals crossing the array. These anomalies are presented, and some concern is given to the effect of these on the event detection and location capability of the array. Tests are made in order to find out whether or not these anomalies can be explained as the effect of a depth varying Moho-discontinuity. It is found that a dipping plane is able to explain 18% of the total variance of these anomalies. A second degree polynomial interface may explain 21% of the variance, while a third degree interface may explain 24%. The conclusion is thus that more complicated models will have to be introduced in order to explain the bulk of these anomalies.

Key words: Time Anomalies — Location Calibration — Crustal Structure — Least Square Interface.

Introduction

It is well known that the observed time delays for signals crossing a seismic array exhibit considerable deviations from the theoretically expected values. Especially for LASA (Large Aperture Seismic Array, Montana, USA) several studies have been made of slowness and travel time anomalies for the purpose of determining the local structure, as well as inhomogeneities in the lower mantle, f.ex., Chinnery and Toksöz (1967); Greenfield and Sheppard (1969); Glover and Alexander (1969); Mack (1969); Zengeni (1970); Iyer (1971); Engdahl and Felix (1971); Davies and Sheppard (1972).

Also for other arrays there have been similar analyses, f.ex., Niazi (1966); Otsuka (1966); Otsuka (1966a); Johnson (1967); Jonson (1969); Corbishley (1970); Husebye *et al.* (1971); Brown (1973); Brown (1973a). At NORSAR few studies of this type have been made: Noponen (1971); Gjøystdal *et al.* (1973). Recently a crustal model has been introduced where wave scattering is caused by small variations in the index of refraction. It is shown that this model is able to explain the large variation in the array data (Aki, 1973; Capon 1974; Dahle, Husebye, Berteussen, and Christofferson, paper in preparation).

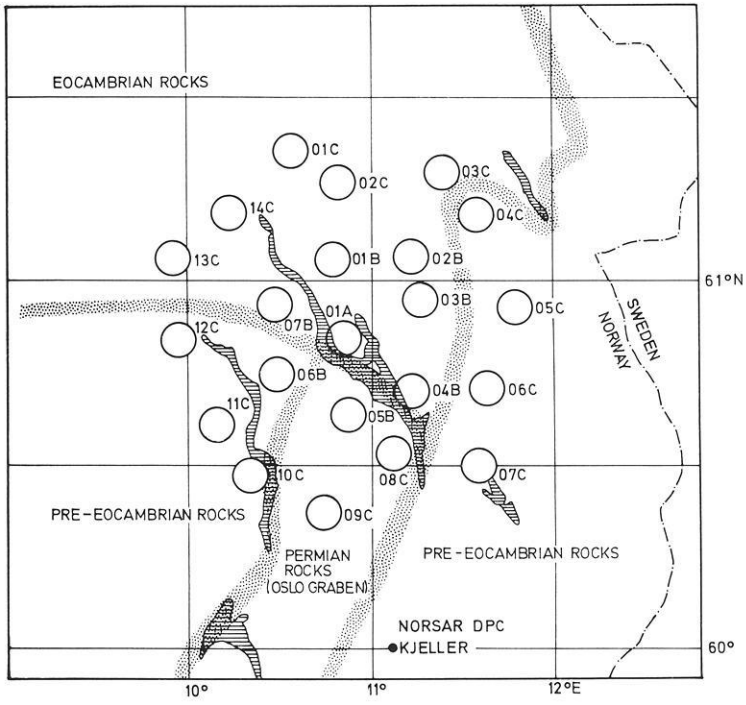

Fig. 1. NORSAR Array configuration. The geological structures in the siting area are briefly outlined

In this paper the *P*-wave travel time and slowness anomalies observed at NORSAR (60.82 N, 10.83 E) will be presented, and some attention will be given to the effect of these on the event location and detection capability of the array.

From other types of data the mantle-crust interface is found to exhibit large elevation differences in this area (Kanestrøm, 1973). The main objective of this paper is therefore to test whether or not the observed anomalies can be explained by either a plane dipping Moho-discontinuity or a Moho which is a curved interface.

DATA

NORSAR has 22 subarrays, each with 6 SP (short period) instruments. The array configuration is shown in Fig. 1. For a more complete description of the array, the reader is referred to Bungum *et al.* (1971).

Because of the time anomalies observed, extensive calibration files had to be established in order to ensure good event location and detection capabilities at the array. The data used in this study is the data which

currently is used for this purpose at NORSAR. The data base has been established by measuring subarray delays on a total of 149 events, all with good signal-to-noise ratio. The delays are found by an iterative cross-correlation procedure (Bungum and Husebye, 1971). Usually a 1.0–3.0 Hz bandpass (third order recursive Butterworth) filter has been applied, but on some of the events a 0.8–2.5 Hz bandpass filter is used. The difference is, however, not believed to be significant in this context (Bungum and Husebye, 1971). A good test of the stability of this method is to measure delays on several events with the same epicenter. For example, for explosions from the same test site it is found that the difference in measured delays is of the order ± 0.02 seconds. For some areas where several events are found close together, the anomalies have been averaged over 2–6 events in order to increase the stability further. The final data set consists of 93 data points, where each point represents one single event or an average over several events.

The anomalies are available in the form:

$$d_{ij} = (\tau_{0_{ij}} - \tau_{c_{ij}}) - (\tau_{0_{rj}} - \tau_{c_{rj}}) \tag{1}$$

$\tau_{0_{ij}}$ is observed delay for subarray i and seismic region j.

$\tau_{c_{ij}}$ is calculated delay for subarray i and seismic region j. The calculated delay is based on NOAA (National Oceanic and Atmospheric Administration) epicenter solutions and a smoothed version of Herrins (1968) tables.

$\tau_{0_{rj}}$ ($\tau_{c_{rj}}$) is observed (calculated) delay at the reference point. In our case we use the average of the delays for this region.

Some of this data is shown as a function of azimuth in Fig. 2. Here as in the rest of the paper only data from *P*-phases have been used. The smooth curves are the sine approximations of the data and will be commented upon later.

The values of the deviations are up to ± 0.7 seconds. When beamforming the array such deviations would have a serious degrading effect on the event detection capability if not corrected for. At NORSAR an interpolation routine is used in order to find the correct delays for each point in slowness space. The SNR (signal-to-noise ratio) gain from applying these corrections has been calculated by analyzing 479 events randomly selected in the period November 1972 until September 1973. It is found that 10% of the events have a gain of 1.5 dB or less, 10% have a gain of 12.5 dB or more, while the median is 6.8 dB. A median of 6.8 dB implies an improvement of 0.34 M_B units in detection capability.

In the calibration system at NORSAR these anomalies are actually split in two. That is, through the 22 subarray delays is fit, in a least square sense, a plane wavefront. This procedure does give a slowness and a direc-

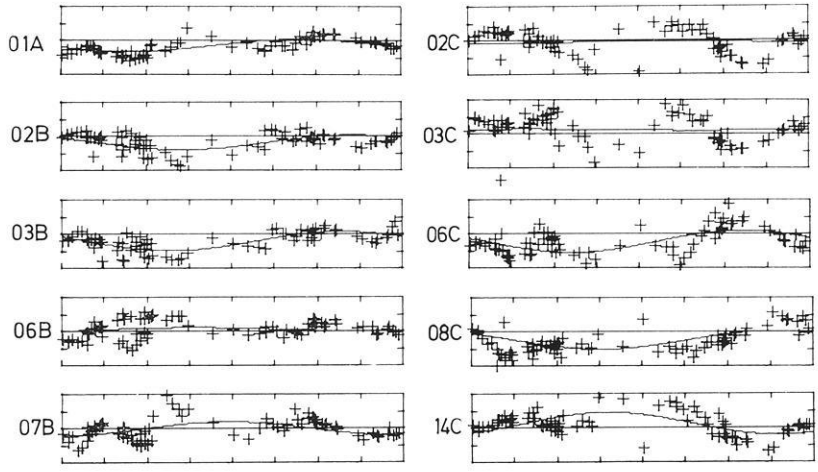

Fig. 2. Observed P wave travel anomalies as a function of (NOAA) azimuth. The vertical axis goes from —0.5 to +0.5 seconds, while the horizontal axis goes from 0 to 360 degrees azimuth. The smooth curve represents the best fit to the sine approximation (Eq. (6)). Only values for 10 of the 22 subarrays are included

tion of approach (azimuth) for the particular event. The location calibration is now defined as the difference in slowness and azimuth between the NORSAR solution and that predicted from the NOAA epicenter location. On Fig. 3 the location calibration vectors for the 93 data points are plotted in slowness space. That is, the tail of the arrow represents the slowness and angle of approach measured at NORSAR, while the head of the arrow represents the corresponding expected values based on the NOAA epicenter solution. The effect of the calibration vectors on the location capability of the array has also been measured, and it is found that for P-phases 10% of the calibrations are greater than 1100 km and the median is 450 km. For the period from April 1972 until March 1973 Bungum and Husebye (1974) have reported a median location difference between NOAA and NORSAR epicenter solutions of 145 km for P-phases, while the 90% level was 490 km. It should also be noted that until 30 November 1972 an older and less complete correction data base was in use. It thus is a safe statement that without the calibrations the event location performance of the array would have been 3 times worse.

Data Interpretation

As mentioned in the introduction, several hypotheses have been put forward in order to explain the types of deviations described here. Mainly they have been interpreted as the single or combined effect of lateral in-

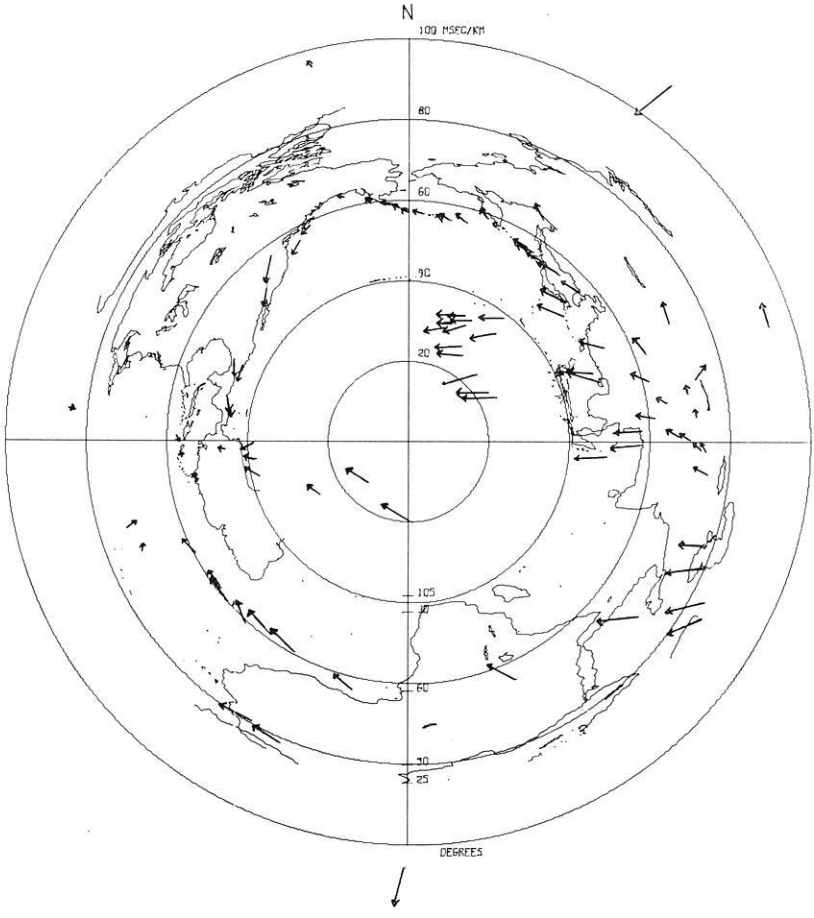

Fig. 3. Location calibration vectors plotted in slowness space. The tail of the arrow represents the observed point, while the head represents the NOAA solution. The contours drawn represent the world map as seen in slowness-space at NORSAR

homogeneities at three different locations along the ray path. One, bending of the ray at the source side of the path, explained as the effect of down-dipping tectonic plates, two, bending of the ray at its deepest (turning) point, and three, inhomogeneities in the crust and upper mantle at the receiver side of the ray path. These last inhomogeneities have usually been interpreted as a Moho interface which deviates from the horizontal plane. More recently scattering caused by small random variations in the index of refraction have been found to be able to explain a large part of the anomalies observed at LASA (Aki, 1973; Capon, 1974). Such studies

have also been performed at NORSAR (Capon and Berteussen, 1973), where the conclusion so far is that the scattering in the upper mantle and crust under NORSAR is too strong to be explained by the Chernov theory (Chernov, 1960). Further studies on this subject are in progress (Dahle *et al.*, paper in preparation).

The mantle-crust interface has been found to exhibit considerable variations in this area (Kanestrøm, 1973). An experiment has therefore been made in order to find out how much of the deviations can possibly be explained by a depth-varying interface located somewhere in the crust or upper mantle beneath NORSAR. To be more specific, this interface will be given a reference depth of 33 km and the *P*-velocities below and above this interface are set to 8.2 and 6.6 km/sec respectively. The aim is then to find the depth varying interface which can explain as much as possible of the deviations which are observed.

Only data from *P*-phases will be used. The deviations will be used as presented in Eq. (1), except that the data will be averaged in intervals of 10 degrees in azimuth. This is to avoid that the cluster of events between azimuth 0 and 90 degrees will have too much influence.

First we will test how much of these anomalies can possibly be explained by a plane dipping interface. A plane wavefront crossing such an interface may change slowness and angle of approach, but will still be a plane wavefront. Therefore such an interface cannot explain any of the wavefront deviations. Using the formulae developed by Niazi (1966) it is possible to calculate the change in slowness and azimuth on a given wavefront when the parameters of the dipping plane are known. Note that in Niazi's paper $\cos(r')$ on page 494 should be replaced by $-\cos(r')$ once in Eq. (6) and two times in Eq. (7) (in the equation for n and the equation for m).

For a certain dipping plane, let dp_{ij} be the travel time anomaly this plane would cause at subarray i for seismic region j. The best plane is then defined as the plane where the parameter

$$R = \sum_{j=1}^{N} \sum_{i=1}^{M} (d_{ij} - dp_{ij})^2 \tag{2}$$

has its minimum. $N = 36$, is number of seismic regions. (The data has been averaged in intervals of 10 degrees spacing in azimuth.) $M = 22$, is number of subarrays d_{ij} is observed travel time anomalies, dp_{ij} is predicted travel time anomalies.

By varying the dip angle and up-dip direction, the plane which gives the minimum value of R has been found. This plane has an up-dip direction of 94 degrees clockwise from north and the dip is 6 degrees. With another velocity contrast the dip angle would of course change. (A contrast of 6.2/8.2 gives for example a dip angle of 4 degrees.) This dipping plane is

Table 1. Table of coefficients for best plane, second degree interface and third degree interface. Per cent reduction in mean squared deviations is also listed for the three models

Model A	$B \cdot 10^3$	$C \cdot 10^3$	$D \cdot 10^3$	$E \cdot 10^3$	$F \cdot 10^3$	$G \cdot 10^6$	$H \cdot 10^6$	$I \cdot 10^6$	$J \cdot 10^6$	% Gain
Plane	−33.0	90.4	22							17.9
2nd degree	−33.0	99.3	−7.9	0.47	−2.0	0.3				21.4
3rd degree	−33.0	222.9	13.1	0.003	−1.55	0.17	33.	−13.5	−51.0 −3.9	24.3

able to explain 17.9% of the squared deviations (Row 1, Table 1). That is, the parameter R (Eq. (2)) is reduced with 17.9% relative to the case where dp_{ij} is uniformly zero.

In this example the interface has been located at the crust-mantle boundary. One is, however, completely free to locate it wherever one should prefer. If, for example, for some reasons the upper mantle is found to be the most likely place the velocity contrast would have to be changed, this would change the dip of the plane, but the updip direction would still be the same. What is most important is, however, that it is not possible to explain more than 17.9% of the variance of the deviations wherever the plane is located.

The equation for the plane used may be written

$$Z = A + B \cdot X + C \cdot Y \tag{3}$$

The values for A, B and C are given in row 1 on Table 1. Our coordinate system is then centered in the array's center with X-axis towards east, Y-axis towards north and Z-axis upwards.

Since a dipping plane cannot satisfactorily explain the deviations, we will go further and try a second degree interface. The equation for this is:

$$Z = A + BX + CY + DX^2 + EXY + FY^2 \tag{4}$$

When the interface can be described in this way, ray-tracing is especially simple and not very time-consuming on a computer. The procedure has therefore been to vary all the coefficients in Eq. (4) systematically. For each set of coefficients conventional ray-tracing has been applied in order to find the deviationas this particular interface would give for our data points. The best interface is then as in the preceding case defined as the interface

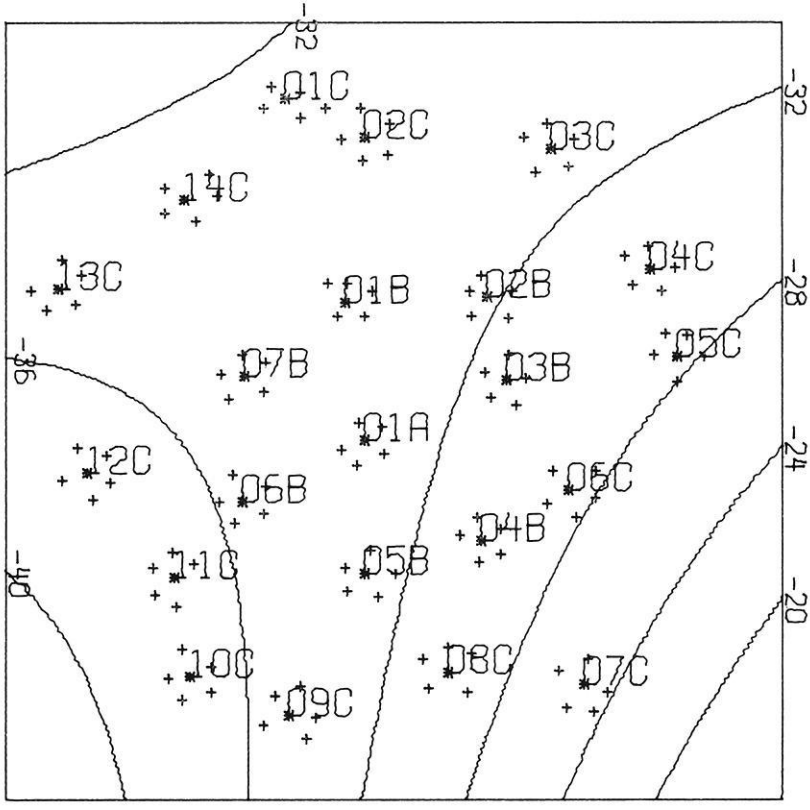

Fig. 4. Depth contours for best 2nd degree interface. $V_C = 6.6$ km/sec, $V_M = 8.2$ km/sec. The NORSAR array configuration is also included

where the sum of the squared differences between predicted and observed deviations has been reduced to a minimum. The coefficients for this surface are listed in row 2, Table 1. As also can be seen from Table 1, this interface is able to explain only 21.4% of the squared deviations. The depth contours for this interface are plotted in Fig. 4. Actually the parameter R in Eq. 2 showed up to be a very well behaved parameter with regard to the coefficients $A, B, \ldots, F$. Some other more efficient minimization procedures could therefore probably have been used with benefit.

The next step was to repeat the above procedure except that this time a polynomial of third order was used. The equation for this is:

$$Z = A + BX + CY + DX^2 + EXY + FY^2 + GX^3 + HX^2Y + IXY^2 + JY^3 \tag{5}$$

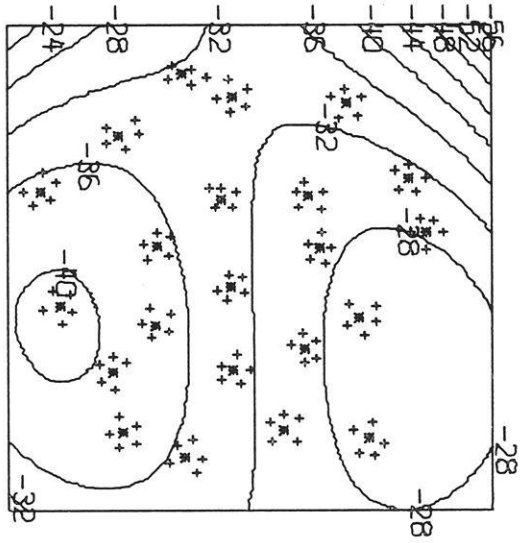

Fig. 5. Depth contours for best 3rd degree interface. $V_C = 6.6$ km/sec, $V_M = 8.2$ km/sec

The coefficients for this interface are listed in row 3 of Table 1. This interface is able to explain 24.3% of the observed squared deviations. The contours for this are drawn in Fig. 5.

Travel time residuals for ordinary stations are commonly approximated with the equation (Bolt and Nuttli, 1966; Nuttli and Bolt, 1969; Lilwall and Douglys, 1969; Payo, 1971).

$$d = A + B \cdot \sin(\sigma + \phi) \tag{6}$$

where σ is station azimuth and the 'early direction' is $(3/4\ \pi - \phi)$. This has been done also for the NORSAR travel time anomalies. The difference from the more common situation is of course that we here are talking of residual between stations instead of absolute travel time residuals. On Fig. 2 the smooth curve is the least squares approximation of the data to Eq. (6). Before performing the approximation, the data as before was grouped and averaged in intervals of 10 degrees in azimuth in order to avoid that the cluster of data between 0 and 90 degrees in azimuth should have too much influence.

The values obtained for A, B and the 'early direction' are listed in Table 2 for the case where only *P*-phase data have been used. In the table are also listed the percentage reduction in mean square deviations by just

Table 2. A, B and early direction for each subarray (see Eq. (6)). Only P-phase data used. Model 1 gives reduction in mean square deviations by using only A, that is, by just subtracting the normalized mean deviations for each subarry. Model 2 gives reduction mean square deviations by using the whole Eq. (6)

Sub. No.	Name	A	B	Early Direction	Model 1 Improvement (%)	Model 2 Improvement (%)
1	01A	—0.07	0.09 ± 0.03	73 ± 23	31.3	56.4
2	01B	—0.05	0.06 ± 0.03	98 ± 32	16.7	27.6
3	02B	—0.09	0.11 ± 0.03	129 ± 18	39.0	61.7
4	03B	—0.10	0.14 ± 0.04	117 ± 16	42.0	77.8
5	04B	—0.08	0.16 ± 0.06	98 ± 23	13.6	39.2
6	05B	—0.10	0.06 ± 0.03	107 ± 35	42.0	48.2
7	06B	0.02	0.03 ± 0.02	320 ± 54	6.9	10.5
8	07B	—0.01	0.10 ± 0.04	356 ± 24	0.2	24.3
9	01C	—0.06	0.10 ± 0.06	308 ± 38	5.9	13.0
10	02C	—0.03	0.01 ± 0.05	26 ± 320	2.2	2.3
11	03C	0.06	0.01 ± 0.05	243 ± 297	8.3	8.5
12	04C	—0.05	0.11 ± 0.04	184 ± 21	9.5	27.9
13	05C	—0.08	0.09 ± 0.04	184 ± 27	14.8	26.0
14	06C	—0.11	0.16 ± 0.05	110 ± 20	28.4	55.8
15	07C	—0.14	0.06 ± 0.05	101 ± 58	31.2	33.8
16	08C	—0.13	0.13 ± 0.04	137 ± 20	36.2	53.8
17	09C	0.07	0.07 ± 0.04	171 ± 35	16.4	23.2
18	10C	0.22	0.12 ± 0.04	242 ± 22	59.3	68.7
19	11C	0.28	0.11 ± 0.03	274 ± 18	77.6	83.6
20	12C	0.26	0.24 ± 0.03	297 ± 8	66.7	91.4
21	13C	0.13	0.32 ± 0.06	313 ± 12	22.9	79.6
22	14C	0.06	0.16 ± 0.05	324 ± 20	8.7	37.7
Total effect					33.8	51.4

subtracting the mean, corresponding to using only A in Eq. (6) (Model 1). The next columns (Model 2) give the percentage reduction in variance by using the whole Eq. (6).

Since the variance of the anomalies changes somewhat from one subarray to another, the total effect of these two models is somewhat different from the average effect on each subarray. From the last row (Table 2) it is seen that by using the whole Eq. (6), the variance may be reduced by 51.4%. This model (2) is the one which best fits the data. For single stations there are several ways to interpret such a model (Nuttli and Bolt, 1969; Lilwall and Douglas, 1969; Payo, 1971). In this case with 22 stations so close together it is difficult to invert the mathematical model into physically reliable structures. For each single subarray the deviations could for example be interpreted as being caused by a plane dipping interface with depth, dip and updip direction given from A, B, and the

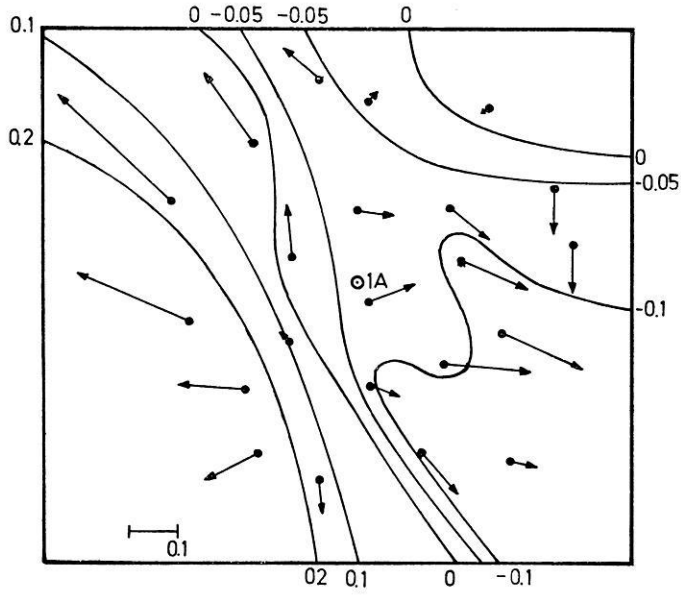

Fig. 6. Contours for average deviations relative to NOAA wavefronts (sec). Only *P*-phase data has been used. The length of the arrow is proportional to B in Eq. (6), while the direction gives the early direction

'early direction'. However, it is quite impossible to combine these planes in a way such that all the 22 equations could be satisfied. It should be noted that model 1, that is, just subtracting a fixed mean value for each subarray, shows a better fit performance than any of the polynomial interfaces tested previously. This model, which has been considered earlier by Gjøystdal *et al.* (1973), may be thought of as representing structural inhomogeneities in the array site area. On Fig. 6 contours for average deviations for *P*-phases are plotted. The arrows on the figure give the 'early direction' and the length of the arrow is proportional to B in Eq. (6).

Discussion

As seen from Figs. 4 and 5, the interfaces found do exhibit such large elevation differences that their geophysical reality is questionable. To increase the order of the polynomial to higher degrees than 3 cannot be done because we then will end up with such a detailed map that simple ray theory may not be used. If the velocity in the crust above the interface is set to 6.2 km/sec, a second degree polynomial found in the same way as described in the above section will be able to explain 24.9% of the squared deviations. The contours for this interface are shown in Fig. 7. The conclu-

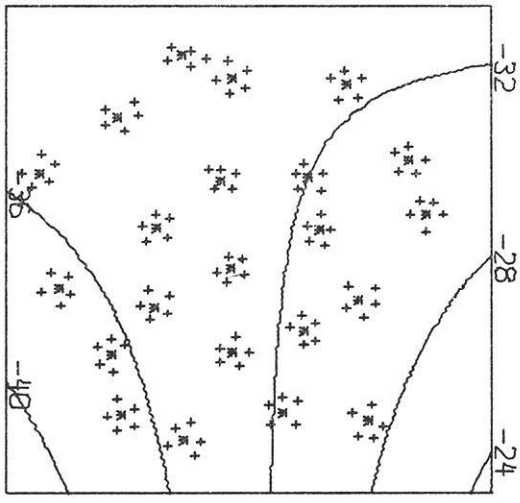

Fig. 7. Depth contours for best 2nd degree interface $V_C = 6.2$ km/sec, $V_M = 8.2$ km/sec

sion is that it is not possible to construct a physically trustworthy interface which is able to explain more than say 25% of the sum of the squared deviations observed at NORSAR. It thus seems that in order to explain the bulk of the deviations observed, other types of models have to be introduced; for example, models where wave scattering and possibly multipathing take a more important part.

To make it quite clear, the Figs. 4, 5 and 7 are not thought of as representing a real interface. The intention with these figures and the section above is to show that the kind of deviations observed exhibit such large variations that they cannot be explained satisfactorily by simple smooth interfaces. Thus, the effect of varying Moho depth cannot be dominant in this data base. In order to say something about the shape of the Moho interface, other types of data therefore have to be used.

Acknowledgement. The NORSAR project is sponsored by the United States Air Force and monitored by the European Office of Aerospace Research and Development, Air Force Systems Command, under Contract Number F-44620-74-C-0001 with the Royal Norwegian Council for Scientific and Industrial Research.

References

Aki, K.: Scattering of P-waves under the Montana LASA. J. Geophys. Res. *78*, 1334–1346, 1973

Bolt, B. A., Nuttli, O.: P-wave residuals as a function of azimuth, I, Observations. J. Geophys. Res. *71*, 5977–5985, 1966

Brown, R. J.: Slowness and azimuth at the Uppsala array. Part 1: Array Calibration and Event Location. Pure Appl. Geophys. *105*, 759–769, (1973)

Brown, R. J.: Slowness and azimuth at the Uppsala array. Part 2: Structural studies. Pure Appl. Geophys. *109*, 1623–1637, 1973a

Bungum, H., Husebye, E. S.: Errors in time delay measurements. Pure Appl. Geophys. *91*, 56–70, 1971.

Bungum, H., Husebye, E. S., Ringdal, F.: The NORSAR array and preliminary results of data analysis. Geophys. J. *25*, 115–126, 1971

Bungum, H., Husebye, E. S.: Analysis of the operational capabilities for detection and location of seismic events at NORSAR, Bull. Seism. Soc. Am., in press, 1974

Engdahl, E. R., Felix, C. P.: Nature of travel time anomalies at LASA. H. Geophys. Res. *76*, 2706–2715, 1971.

Gjøystdal, H., Husebye, E. S., Rieber-Mohn, D.: One-array and two-array location capabilities, Bull. Seism. Soc. Am. *63*, 549–569, 1973

Glover, P., Alexander, S. S.: Lateral variations in crustal structure beneath the Montana LASA. J. Geophys. Res. *74*, 505–531, 1969

Greenfield, R. J., Sheppard, R. M.: The Moho depth variations under the LASA and their effect on DT/dΔ measurements. Bull. Seism. Soc. Am. *59*, 409–420, 1969

Herrin, E., (Chairman) Seismological table for P-phases, Bull. Seism. Soc. Am. *58*, 1193–1241, 1968

Husebye, E. S., Kanestrøm, R., Rud, R.: Observations of vertical and lateral P-velocity anomalies in the earth's mantle using the Fennoscandinavian continental array. Geophys. J. *25*, 3–16, 1971

Iyer, H. M.: Variation of apparent velocity of teleseismic P-waves across the Large Aperture Seismic Array (LASA), Montana, J. Geophys. Res. *76*, 8554–8567, 1971

Capon, J.: Characterization of crust and upper mantle structure under LASA as a random medium, Bull. Seism. Soc. Am., in press, 1974

Capon, J., Berteussen, K. A.: Semiannual Technical Summary Report to the Advanced Research Projects Agency, Mass. Inst. Tech., Lincoln Lab., Cambridge, Mass., USA, December 1973

Chernov, L. A.: Wave Propagation in a Random Medium, Translated by R. A. Silverman. New York: McGraw-Hill Book Company 1960

Chinnery, M. A., Toksöz, M. N.: P-wave velocities in the mantle below 700 km. Bull. Seism. Soc. Am. *57*, 199–226, 1967

Corbishley, P. J.: Multiple array measurements of the P-wave travel time derivative. Geophys. J. *19*, 1–14, 1970

Davies, D., Sheppard, R. M.: Lateral heterogeneity in the earth's mantle. Nature *239*, 318–323, 1972

Iyer, H. M., Healy, J. H.: Teleseismic residuals at the LASA USGS extended array and their interpretation in terms of crust and upper mantle structure. J. Geophys. Res. *77*, 1503–1527, 1972

Johnson, L. R.: Array measurements of P velocities in the upper mantle. J. Geophys. Res. *72*, 6309–6324, 1967

Johnson, L. R.: Array measurements of P velocities in the lower mantle, Bull. Seism. Soc. Am. *59*, 973–1008, 1969

Kanestrøm, R.: A crust-mantle model for the NORSAR area. Pure Appl. Geophys. *105*, 729–740, 1973

Lilwall, R. C., Douglas, A.: Estimation of P-wave travel times using the joint epicenter method. Geophys. J. *19*, 165–181, 1970

Mack, H.: Nature of short-lived P-wave signal variations at LASA. J. Geophys. Res. *74*, 3161–3170, 1969

Niazi, M.: Corrections to apparent azimuths and travel time gradients for a dipping Mohorovicic discontinuity. Bull. Seism. Soc. Am. *56*, 491–509, 1966

Noponen, I.: Analysis of event location errors using arrays in Scandinavia. Proc. from the seminar on seismology and seismic arrays. NTNF/NORSAR, Kjeller, Norway, 1971

Nuttli, O. W., Bolt, B. A.: P-wave residuals as a function of azimuth, 2, Undulations of the mantle low-velocity layer as an explanation. J. Geophys. Res. *74*, 6594–6602, 1969

Otsuka, M.: Azimuth and slowness anomalies of seismic waves measured on the central California seismographic array, Part 1, Observations. Bull. Seism. Soc. Am. *56*, 223–239, 1966

Otsuka, M.: Azimuth and slowness anomalies of seismic waves measured on the central California seismographic array, Part 2, Interpretation. Bull. Seism. Soc. Am., *56*, 655–675, 1966a

Payo, G.: P-wave resicuals at some Iberic stations and deep structure of South-Western Europe. Geophys. J. *26*, 481–497, 1971

Zengeni, T. G.: A note on azimuthal correction for $dT/d\Delta$ for a single dipping plane interface. Bull. Seism. Soc. Am., *60*, 299–306, 1970

K. A. Berteussen
NTNF/NORSAR
Post Box 51
N-2007 Kjeller
Norway